Design, construction and robust validation of a germicidal device based on UV irradiation: a necessity for hospital disinfection in the COVID-19 era

I. Martínez-Ramírez[a], C. Cruz-Cruz[b,c], A. López-Ornelas[b,d], E. Mariano Durán-Manuel[b,c], E. Estudillo[e], I. Velasco[e,f], M. Ángel Loyola-Cruz[b], P. Gutiérrez Zayas-Bazán[a], J. López López-Vargas[a], Y. Godínez-Cruz[a], M. Tufiño-Velázquez[a], G. Ibáñez-Cervantes[b,c], J. M. Bello-López[b,**], and G. Silverio Contreras-Puente[a,*]

[a]*Escuela Superior de Física y Matemáticas, Instituto Politécnico Nacional, Ciudad de México, Mexico.*
[*]*e-mail:gscp1953@gmail.com*
[b]*Hospital Juárez de México, Ciudad de México, México.*
[**]*e-mail: juanmanuelbello81@hotmail.com*
[c]*Sección de Estudios de Posgrado e Investigación, Escuela Superior de Medicina, Instituto Politécnico Nacional, Ciudad de México, México.*
[d]*Hospital Nacional Homeopático, Hospitales Federales de Referencia, Ciudad de México, Mexico.*
[e]*Laboratorio de Reprogramación Celular, Instituto Nacional de Neurología y Neurocirugía "Manuel Velasco Suárez", Ciudad de México, Mexico.*
[f]*Instituto de Fisiología Celular, Neurociencias, Universidad Nacional Autónoma de México, Ciudad de México, Mexico.*

Received 1 February 2023; accepted 9 May 2023

Pandemic by SARS-CoV-2 has revealed the importance of disinfection methods to pathogens of medical importance being detectable and infective after several hours on contaminated surfaces, including medical devices. The aim of this work was to design, construct, and validate a UVC light irradiator which operates in the short wavelength region (200 to 320 nm). We studied the effectiveness of the irradiator through *in vitro* disinfection to eliminate pathogens such as SARS-CoV-2, ESKAPE bacteria and fungi in biofilm and planktonic forms. It was observed that doses of 0.25 J/cm^2 (10 s of exposure to UVC light) annihilates 100% of ESKAPE bacteria and fungi in planktonic form. Through biofilm formation induction assays of these microorganisms showed resistance to treatment with UV light; however, their viability was not detected after 20 s of exposure (via confocal microscopy). A 100% of reduction for SARS-CoV-2 was reached after 120 s of exposure. This evidence shows the need to employ emerging methods of disinfection of surfaces and medical devices since these are potential vehicles for transmitting pathogens. The advantages of using UV light as an emergent disinfection method in the era of COVID-19 are discussed.

Keywords: UV light; SARS-CoV-2; ESKAPE bacteria; fungi; disinfection.

DOI: https://doi.org/10.31349/RevMexFis.70.010901

1. Introduction

The pandemic caused by the new coronavirus SARS-CoV-2, has exposed the importance of disinfection methods. The UV light has been employed as an alternative powerful method to eliminate several biological pathogens, including the SARS-CoV-2 virus on surfaces [1-6]. Although airborne is the main route of transmission of the coronavirus, the deposition of the virus on inert surfaces also becomes relevant [7-9,13-16]. Previous studies report that the SARS-CoV-2 virus and bacterial pathogens of medical importance are detectable and infective after several hours on contaminated surfaces. SARS-CoV-2 and other coronaviruses can persist infectious under environmental conditions within the first 72 hours if deposited on common non-porous surfaces such as stainless steel, plastic, and glass [12-19]. In the case of bacterial pathogens, they remain in medical devices employed in intensive care units of COVID-19 patients [20].

Moreover, the spread of new and devastating pathogens, such as the H1N1 virus, MERS, or SARS-CoV-2, requires more scientific knowledge on disinfection, especially on surfaces and medical devices [21,22]. Disinfection methods for bacterial, fungi, and viral pathogens include highly invasive gases and plasmas such as hydrogen peroxide (H_2O_2) and ozone (O_3) [23,24]. These methods allow the reuse of medical devices to protect health personnel (N95 masks and biosecurity gowns) and materials used in surgery rooms [5,25], showing the need for emerging methods of disinfection surfaces and medical devices since these are potential vehicles for transmitting pathogens [19,26,27].

The effectiveness of ultraviolet (UV) light for disinfection of medical infrastructures such as operating theatres, consulting rooms, and other critical areas is widely known [28]. The design of new UV light devices that effectively disinfect is an imminent necessity. For this purpose, we report the design, construction, and robust validation of a UVC light irradiator system equipped with eight lamps with low-pressure mercury emission, radiometer, timer, and humidity sensor. We studied its effectiveness through *in vitro* disinfection tests for the elimination of pathogens of medical importance: the SARS-CoV-2 virus, ESKAPE bacteria, and *C. Krusei*, described as a causative agent of pneumonia in COVID-19 patients [29]. Implications and advantages of using UVC light to disinfect medical devices in the COVID-19 era are analyzed and discussed.

2. Material and methods

2.1. Ethical aspects

The institutional Committee of Research, Ethics, and Biosafety from Hospital Juárez de México (HJM) approved the protocol under the registration number HJM 0789/20-R following the Regulation of the General Health Law on Research for Health [30].

2.2. Design/construction of short-wave UVC light irradiation system (Patent pending)

For the disinfection tests we designed disinfection equipment based on the irradiation of short-wave UVC light. The UVC emission is in the wavelength region of 200 to 320 nm, which induces photochemical damage in vital biomolecules. The electromagnetic radiation wavelength emitted from the system is 254 nm by mercury lamps, with a surface energy density ranging from 0.5 to 1.8 J/cm^2. The equipment has a timer for the operation of 45, 60, 90, and 120 s. However, it can operate in a shorter time of irradiation.

Device dimensions are $35 \times 30 \times 28$ cm, with a central reticulated sample plate. The power per unit area, measured with a radiometer integrated into the equipment in the center of the sample plate, is about 25 mW/cm^2. The irradiance measurement is based on photocurrent delivered by a UVC Schottky-type photodiode with a linear photocurrent output of 39 nA per mW/cm^2 at 254 nm of wavelength, coupled with a high-performance operational amplifier circuit, configurated as a current-to-voltage converter. The controller thus uses the measured voltage value to calculate the surface energy density (J/cm^2), depending on the irradiation time. The system has eight Hg-lamps model TUV-T5 at low gas pressure and the quartz glass of the lamp absorbs the UVC radiation at 185 nm that produces O_3. Each lamp consumes 16 W, with a radiant flux of 4 W; the model can have more lamps installed.

Moreover, the equipment also has an Adafruit Industries humidity-temperature capacitive sensor [31] that provides additional information on the disinfection conditions. Other circuits include the primary electrical source, with an alternating current (AC) to direct current (DC) converter to operate the controller, the secondary electric source, the air-exhausting ventilator, and the main switch of the lamps. The system has an optically protected door made with solid polycarbonate. The inner walls are made of stainless-steel mirror-type sheets, thus reflecting the UVC- radiation during the operation. Additionally, it has a microswitch that turns off the lamps in case of a sudden or purposed door aperture. The UVC system and the main external accessories are shown in Fig. 1a), such as the outer aluminum frames; the display, manual timer and starting button are located on the upper part from left to right. The on/off switch is located in the last right position.

Figure 1b) shows a detailed schematic of the system's side view and the device's various parts, including the disinfection chamber with the grid for placing the samples during UVC irradiation. Four UVC lamps are at the bottom and the other four at the top; these lamps are separated at a distance $A = 5$ cm from each other. The distance from the upper lamps to the sample is $U = 9$ cm and the distance from the lower lamps to the sample is $B = 7$ cm; the distance between the grid bars is $a = 1.4$ cm, and the lamps are separated by $v = 2$ cm of stainless-steel sheets (SU, SB, and SR). Additionally, the diameter of the UVC lamp is 1.6 cm and its length is 28.8 cm, and the diameter of the grid bars is 0.3175 cm. Finally, the sensor kit (KS), control buttons (CB), and the fan (F) behind the disinfection chamber are shown. Figure 1c) shows the graph of the spectral emission of the mercury lamps in units of mW/m^2, the most intense corresponding to the 254 nm wavelength, followed by a series of less intensity located in the range from 300 to 500 nm. Figure 1d) illustrates the iso-irradiance curves measured in the central plate of the equipment [Fig. 1b)]; it was determined with a radiometer at a net of 600 points (20×30) along the grid surface and the curves were calculated using the Mathlab software. The grid-center has a surface energy density of 3 J/cm^2, obtained for a particular irradiation time of 120 s, whereas for the minimum time of 45 s, a value of 1.1 J/cm^2. The mean irradiance in the grid is 20 mW/cm^2.

TABLE I. Bacterial, fungi, and viral strains used in this study.

Strains	Isolation source	Reference
Acinetobacter baumannii	Mechanical ventilator	[25]
Klebsiella pneumoniae	Mechanical ventilator	
Pseudomonas aeruginosa	Mechanical ventilator	
Citrobacter freundii	Vital signs monitor	[13]
Staphylococcus aureus	Oxygen source	
Candida krusei	COVID-19/NAV patient	This work
SARS-CoV-2	COVID-19 patient	This work

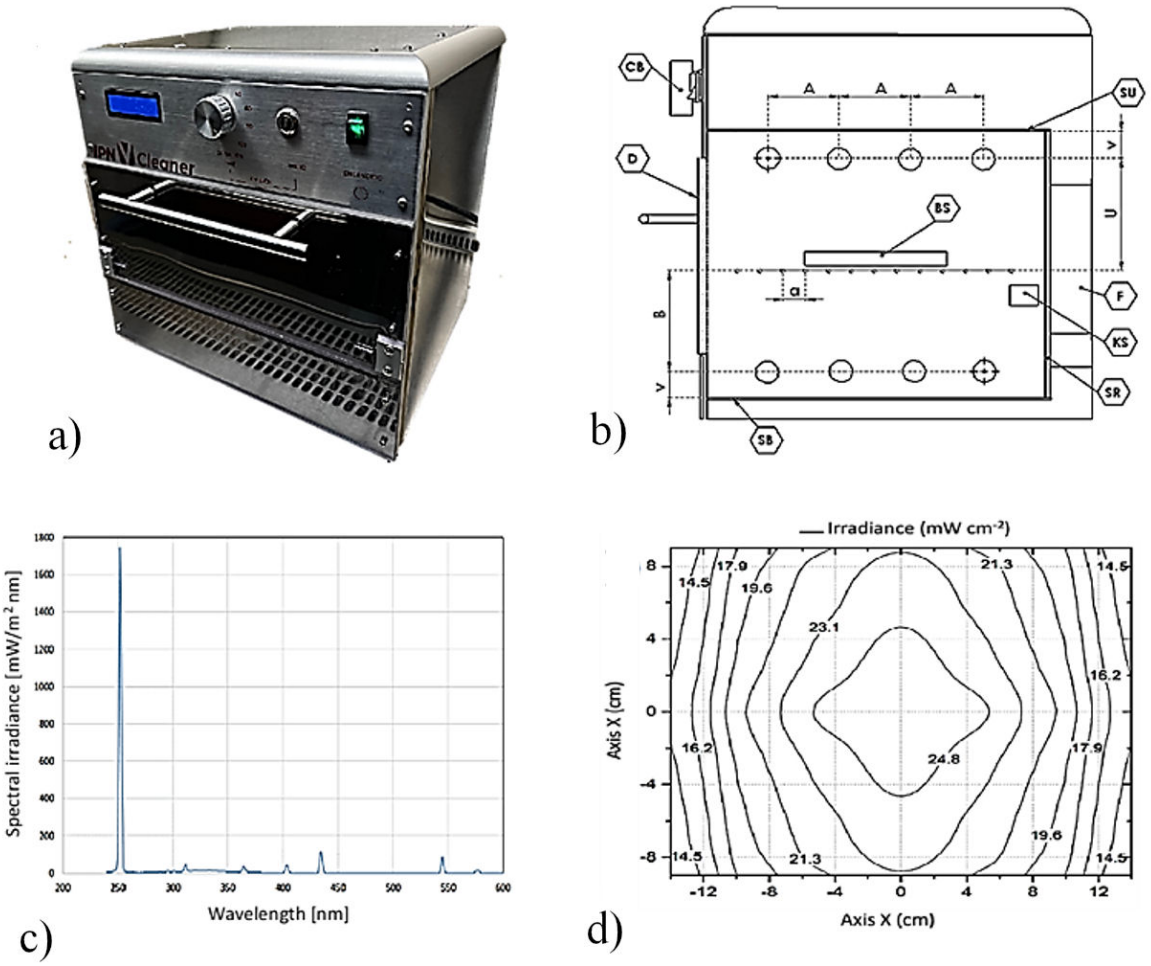

FIGURE 1. a) The system's photograph by isometric perspective showing; display, manual timer, starting button, on and off button, from left to right, respectively. b) Side view of the system and the various parts of the device; the door (D), four UVC lamps are in the lower part and the other four in the upper part, stainless steel sheets (SU, SB, and SR), kit of humidity, temperature, and radiometer sensors (KS), control buttons (CB) and the fan (F), which is behind and in the disinfection chamber. Additionally, the position of the biological sample (BS) is shown. c) Typical spectral irradiance of the Hg-lamps installed in the system. d) Iso-irradiance curves are determined in the system grid.

2.3. Validation of device UVC system

2.3.1. Bacterial, fungi, and viral strains

Virus, bacterial, and fungi strains used in this study are in Table I. Bacterial strains were reported by Duran-Manuel *et al.*, 2021 [20] and Cureño-Diaz *et al.*, 2021 [32]. They were genetically identified by 16S rRNA gene sequences (bacteria) and mass spectrophotometry "MALDI-TOF" (fungi). *Candida krusei* fungi were isolated from a COVID-19 patient and ventilator-associated pneumonia (VAP). Strains were characterized to determine mature biofilm-forming capacity by the violet crystal method.

2.3.2. Manipulation of SARS-CoV-2 virus

Nasopharyngeal exudate was collected in virus preservation solution (DOUBANG^{TM} disposable, Biocomma) from a symptomatic patient admitted to the intensive care unit of the HJM to detect SARS-CoV-2 virus, according to the Berlin protocol. Multiplex amplification (E, $RdRp$, and $RNAse\ P$ genes) was performed by using the WoV19 Kit (Genes2 Life, Irapuato Guanajuato, Mexico). In RT-qPCR assays, positive controls provided by the "Instituto de Diagnóstico y Referencia Epidemiológicos" (InDRE-México) for the E, $RdRp$, and $RNAse\ P$ genes were used. Linear regression was performed between the cycle threshold value (Ct-value) and the log10 of the copy number for SARS-CoV-2. The final load of SARS-CoV-2 used in disinfection assays was 2.5×106 copies/50 μl.

2.3.3. Preparation of ESKAPE bacteria and fungi in planktonic form

Strains were inoculated in LB-broth under agitation at 200 rpm at 37°C for 24 h and 28°C during 48 h, respectively. The cultures were adjusted to 106 CFU/50 μl using a Spectrophotometer 3000 SmartSpec^{TM} flow (BIORAD) at 600 nm and diluted to obtain 10^2, 10^3, 10^4, 10^5, and 10^6 CFU/50 μl. Microbial dilutions were spread onto LB-agar and incubated

for the CFU counting to confirm the bacterial and fungi densities. Bacterial and fungi planktonic suspension forms were subjected to UVC light treatment.

2.3.4. Germicidal activity of the UVC irradiator system on bacteria and fungi in planktonic form

Loads of planktonic forms of bacteria and fungi were spread (10^2, 10^3, 10^4, 10^5, and 10^6 CFU) onto LB agar (per triplicate). UVC light treatments using plastic Petri dishes, 5 cm in diameter, without lid, placed in the central area of the equipment were conducted using the system at different exposure times (5, 10, 20, 45, 60, 90, and 120 s) to obtain 0.125, 0.25, 1.125, 1.5, 2.25 and 3 J/cm^2 (UVC doses) respectively. Once the UVC light treatments were completed, Petri dishes were incubated at 37°C for 48 h (bacteria) and 28°C for 72 h (fungi). Controls (without UVC light treatment) were included.

2.3.5. In vitro formation of mature biofilms of bacteria ESKAPE and fungi

Mature biofilms of ESKAPE strains were prepared according to Rodríguez-Baño *et al.*, (2008) [33]. ESKAPE bacteria was cultured in 3 ml of LB broth with shaking at 37°C for 24 h at 200 rpm. Cultures were subcultured one more time in 3 ml of LB broth in the same conditions. Bacterial cultures were centrifuged, and cold isotonic saline solution was added to the bacterial pellet and adjusted to a 0.5 McFarland nephelometer. On the other hand, fungi mature biofilm was prepared according to Gulati *et al.*, (2018) [34]. Bacterial and fungi suspension (0.5 *et al.*, McFarland) was inoculated (10 μl) in BHI-broth (250 μl) on plastic coverslips of 13 mm (Thermanox®, Rochester, NY, USA) into wells of a cell culture plate (per triplicate). The plates were sealed and incubated at 37°C for 48 h (bacteria) and 28°C for 72 h (fungi). Non-adherent cells were removed from the microplate by aspiration. Wells plates were gently washed with 1× PBS (pH 7.4) and were subjected to UVC light treatment.

2.3.6. Treatment of mature biofilms of bacteria and fungi with the UVC system

UVC light treatment of mature biofilms using plastic Petri dishes, 5 cm in diameter, without lid, placed in the central area of the equipment was conducted at exposure times of 5, 10, 20, 45, 60, 90, and 120 s to obtain 0.125, 0.25, 1.125, 1.5, 2.25 and 3 J/cm^2 (UVC doses) respectively. Biofilms treated were fixed using 4% paraformaldehyde and were washed with sterile 1× PBS and were stained using fluorescent dyes to identify live and dead bacteria and fungi by fluorescence microscopy. Syto9/PI-stained biofilms allowed for monitoring the viability as a function of the membrane integrity. Cells with a compromised membrane were red, whereas cells with an intact membrane were green. Images were acquired on a Cytation 5 Cell Imaging Multimode Reader (Agilent, CA, United States) with an objective of 20x. Viable and non-viable cells were observed at 488 nm and 543 nm, respectively, and counted using the Gen5 software.

2.3.7. Treatment of SARS-CoV-2 with UVC irradiator system

SARS-CoV-2 virus (2.5×106 copies/50 μl) was inoculated on plastic Petri dishes (without lid) with dimensions of 50×15 mm and placed in the central zone of the equipment. UVC light treatments of SARS-CoV-2 were conducted at exposure times of 5, 10, 20, 45, 60, 90, and 120 s to obtain 0.125, 0.25, 1.125, 1.5, 2.25 and 3 J/cm^2 (UVC doses) respectively. The UVC-treated samples (per triplicate) were subjected to detection of SARS-CoV-2 by RNA extraction and amplification of E, $RdRp$, and $RNAse\ P$ genes. The Cycle Threshold (Ct) values obtained by RT-qPCR were interpolated in the viral load curve to determine the SARS-CoV-2 particles detected after UV disinfection [35].

2.3.8. Mathematical calculations

Residual ESKAPE bacteria and fungi and SARS-CoV-2 virus after UVC disinfection were registered, and Logarithmic Reduction Values (LRV) were calculated by using the following equation:

$$L = \mathrm{Log}_{10}(A) - \mathrm{Log}_{10}(B), \tag{1}$$

where L is the LRV, A is the pathogen (CFU of bacteria, fungi, and viral copies) before disinfection, and B is the number of the pathogen (CFU of bacteria or fungi or viral copies) after UVC disinfection. Additionally, the Percent Reduction Values (PRV) were calculated by using the following equation:

$$P = \left(\left[1 - 10^{-L}\right][100]\right), \tag{2}$$

where P is the PRV, and L is the LRV.

3. Results

3.1. The UVC irradiator system has bactericidal and fungicidal activity on planktonic forms

As an initial approach to studying the effects of UVC light on ESKAPE bacteria and fungi, we evaluated the germicidal activity of the UVC light at 40, 60, 90, and 120 s of irradiation in the planktonic forms of *A. Baumannii et al.*, (Table I). These irradiation times correspond to the four settings on the system device. Figure 2 shows that at 40 s of UVC light irradiation, there is a bactericidal activity (100% of death) for all strains at all microbial densities tested in planktonic form. The absence of living bacteria and fungi (0 CFU) by plate culture with LRV = 6, 5, 4, 3, and 2 logs and PRV = 100% after UVC light treatment at 60, 90, and 120 s of irradiation confirmed this (Fig. 2), indicating that UVC light possesses bactericidal and fungicidal activity. To determine the dependent

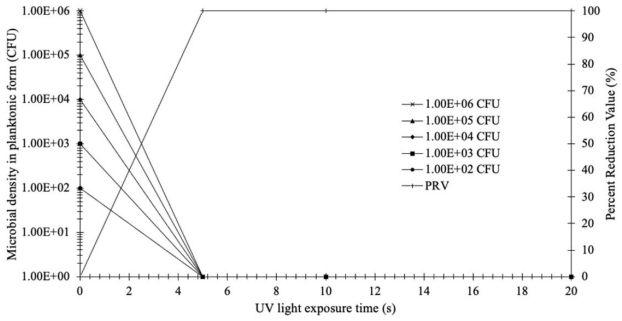

FIGURE 2. Curves of Percent Reduction Values versus microbial density after UVC light exposure with the UVC irradiator system on bacteria ESPAKE in planktonic forms.

variables studied "irradiation time *versus* microbial load," *in vitro* disinfection tests were carried out using short irradiation times (5, 10, and 20 s).

The results showed that after 5 s of irradiation treatment to the strains of *A. Baumannii and C. Freundii*, an LRV of 5.84 and S. aureus of 4.94 were obtained, equivalent to PRV of 99.99%. For the remaining strains (bacteria and fungi), the shortest exposure times to UVC light gave a PRV=100% (Fig. 2).

3.2. The UVC irradiator system has bactericidal and fungicidal activity on mature biofilms

Demonstrated the effectiveness of UVC light on planktonic forms of ESKAPE bacteria and fungi; the efficacy of UVC

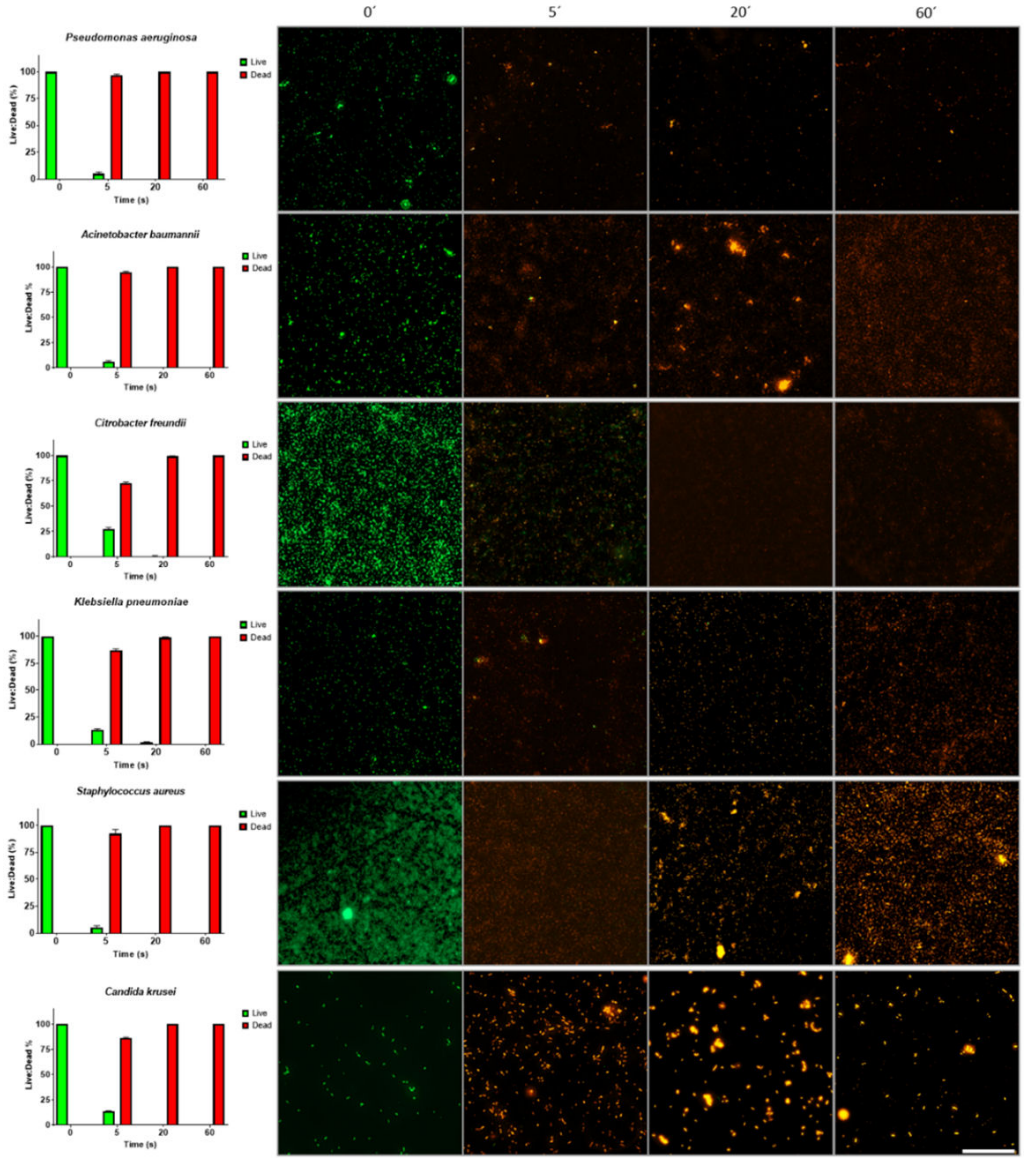

FIGURE 3. Live/Dead staining assay of ESKAPE bacteria and *Candida Krusei* mature biofilms before and after UVC light treatment with the system at 0 (Control), 5, 20, and 60 s. Live bacteria/fungi were stained green and dead bacteria/fungi were stained red. Bars are means $\pm$ Standard error. Scale bar = 10 μm.

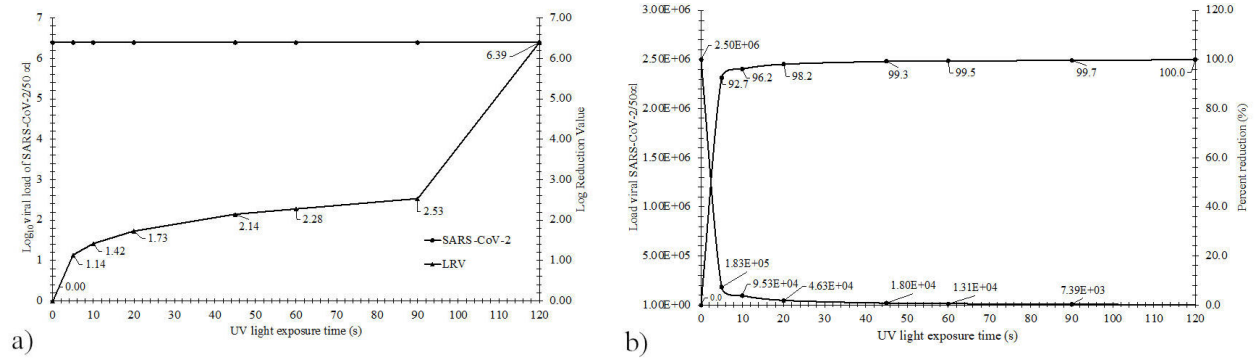

FIGURE 4. The viricidal activity of UVC light against SARS-CoV-2 virus with the UVC irradiator system at 0 (Control), 5, 10, 20, 46, 60, 90, and 120 s. a) Log10 Viral load of SARS-CoV-2 versus Logarithmic Reduction Value (LRV). b) Log10 Viral load of SARS-CoV-2 versus Percent Reduction Value (PRV).

light irradiation on killing mature biofilms during 5, 20, and 60 s of exposure was analyzed. Mature biofilms of ESKAPE bacteria and fungi exposed to UVC revealed the effectiveness of the treatment against these biological structures (from the first 5 s exposure to UVC light). Comparisons with controls and the treated biofilms showed that live cells (stained green) were identified after 5 s exposure to UVC light compared to irradiation experiments with planktonic forms. A close relationship was observed between exposure to UVC light and bacterial viability. *Acinetobacter Baumannii and S. Aureus* at 5 s of irradiation had a death percentage of 94.75, and from 20 to 60 s irradiation, no live bacteria (stained red) were detected. In the case of *K. Pneumoniae*, death percentages of 87 and 98.75% were observed after UVC light irradiation of 5 and 20 s, respectively. At 60 s of UVC light exposure, live *K. Pneumoniae* cells were not detected. *P. Aeruginosa* showed that after 5 s of UVC light treatment, only 5% of live bacteria was detected. After 20 and 60 s, live bacteria was not detected. Contrastingly, *C. Freundii* showed resistance to UVC light after 5 s of UVC irradiation. Percentages of 27.5 and 0.75 live bacteria were detected after UV light treatment. Sixty seconds of UVC light treatment were sufficient to kill all bacterial populations in mature biofilm. Finally, *C. Krusei* showed that after 5 s of UVC light irradiation, 13.5% of cells stained green, and after a 20 s treatment all mature biofilm was killed (Fig. 3).

3.3. The system has virucidal activity on SARS-CoV-2

The biocide activity of UVC light on SARS-CoV-2 was analyzed in samples of clinical origin with loads of $2.5 \times 10^6/50$ μl inoculated on crystalline plastic plates and subjected to different exposure times to UVC light. The detection by RT-qPCR of the virus after the disinfection treatments showed that the burden of SARS-CoV-2 was considerably reduced from the first 5 s exposure to UVC light (LRV = 1.14/PRV = 92.7%). In the disinfection trial for 120 s, an LRV of 6.39 was reached, equivalent to a PRV of 100% (Fig. 4).

4. Discussion and conclusions

Due to the current pandemic SARS-CoV-2 coronavirus, there is the appearance of highly infectious variants along with the impact of bacterial and fungal infections in patients with COVID-19; arising the need to implement strategies that limit its spread [36-38]. Disinfection methods are an emerging alternative to this problem since germicidal agents restrict the spread of pathogens of medical interest. The efficiency of UVC light as a germicidal agent against viruses, bacteria, parasites, filamentous fungi, and yeast has been widely demonstrated [39,42]. However, to our knowledge, only some studies evaluate UVC light irradiators against another type of pathogens of clinical relevance [43,44], in our research besides SARS-CoV-2 we report studies on pathogens causing pneumonia and opportunistic as fungi.

Here we report the design, construction, and robust validation of the UVC irradiator device system through *in vitro* disinfection tests against SARS-CoV-2, bacterial and fungal pathogens related to infections related to the assistance. The results on reducing the microbial loads employed (planktonic and biofilm) confirm the effectiveness of the UVC irradiator system, so it can potentially be used for disinfection purposes of instruments and protective equipment in patients suspected and confirmed of COVID-19 or who undergo bacterial or fungal infectious processes. The germicidal efficiency of the system comes from its operation in the short wavelength range of 200 to 320 nm (UVC region), which according to medical and biological studies, eliminates a wide diversity of pathogens, so in principle, our device presented here is effective and efficient against specific bacteria, fungi, and viruses, such as the novel coronavirus SARS-CoV-2 [45,46]. The 32 watts from the eight Hg UVC lamps produce an average surface energy density at 60 s of 1 J/cm^2 in the 600 cm^2 of the sample rack. Previous studies show that unless this energy is used, it meets the requirements to be used as a disinfecting agent without compromising the structure of materials subjected to textile disinfection, such as polypropylene [47]. It has also been shown that less than 1 J/cm^2 of surface energy density (0.5 J/cm^2) is sufficient to reduce the SARS virus significantly [48]. This study demonstrated logarithmic reduc-

tions in SARS-CoV-2 like those presented in this work using this energy (Fig. 4).

Concerning the disinfection of seedling microbial agents, irradiation assays showed significant reductions in all densities tested after the first 5 s of exposure to UVC light. Logarithmic decay in the recovery of microorganisms and the abrupt increase in PRV confirm the efficiency of the device (Fig. 2). These data are consistent with those previously reported by other authors with significant logarithmic reductions of up to 3 and 2, with doses of 250 mJ/cm^2 and 60 mJ/cm^2 using bacterial models such as *Bacillus subtilis* spores and SARS-CoV-2 immersed in human saliva [49,50]. Resistance to UVC light was not detected, as has already been reported in several strains of *L. Pneumophila*, a pathogen that causes respiratory infections by inhalation of contaminated aerosols. This work shows that although they are genetically identical strains of *L. Pneumophila*, some have some degree of resistance to UVC irradiation [51]. One of the resistance mechanisms that pathogens have developed to evade the action of antimicrobials and disinfectants, including chemical and physical agents, are biofilms [52,53]; their presence in medical devices has gained relevance due to their difficult eradication through traditional disinfection methods [32]. We consider that these biological structures could be involved in UVC light resistance. UVC irradiation treatments on these biofilms showed some degree of resistance in the first 5 min of exposure (Fig. 3) compared to disinfection assays with seedling forms of the pathogens analyzed (Fig. 2).

The UVC irradiator system has all the necessary characteristics to be potentially used for disinfection of instruments, germicidal protection equipment, and others that have been contaminated during use. Disinfection methods are one of the main strategies to contain the current COVID-19 pandemic.

Acknowledgments

We acknowledge to "Secretaria de Investigación y Posgrado of IPN" for the economic support to the development of the UVC irradiator system. This study was partially funding by the project "CONACyT 313771: Análisis del efecto del ozono sobre SARS-CoV-2 como alternativa de producto desinfectante en equipos de protección del personal de salud de alta demanda" and funding of the 02 budget (years 2020, 2021) of the "Hospital Juárez de México" and partially funded by the CONACyT 300461 to Instituto Nacional de Neurología y Neurocirugía Manuel Velasco Suárez.

1. K. Bispo-dos-Santos *et al.*, Ultraviolet germicidal irradiation is effective against SARS-CoV-2 in contaminated makeup powder and lipstick. *J. Photochem Photobiol.* **8** (2021) 100072.
2. S. Srivastava, X. Zhao, A. Manay, Q. Chen, Effective ventilation and air disinfection system for reducing coronavirus disease 2019 (COVID-19) infection risk in office buildings. *Sustain Cities Soc*. (2021) 75.
3. F. P. Sellera, C. P. Sabino, F. V. Cabral, and M. S. Ribeiro, A systematic scoping review of ultraviolet C (UVC) light systems for SARS-CoV-2 inactivation. *J. Photochem. Photobiol*. **8** (2021) 100068.
4. E. Criscuolo *et al.*, Fast inactivation of SARS-CoV-2 by UV-C and ozone exposure on different materials. *Emerg Microbes Infect*. **10** (2021) 206-10.
5. S. Narayanan *et al.*, Disinfection and Electrostatic Recovery of N95 Respirators by Corona Discharge for Safe Reuse. *Environ Sci Technol*. **55** (2021) 15351-60.
6. Y. Huang, S. Xiao, D. Song, Z. Yuan, Evaluating the virucidal activity of four disinfectants against SARS-CoV-2. *Am J Infect Control*. **50** (2022) 319-24.
7. P. Shrestha, J. W. DeGraw, M. Zhang, X. Liu, Multizonal modeling of SARS-CoV-2 aerosol dispersion in a virtual office building. *Build and Environ.* **206** (2021) 108347.
8. P. F. Horve, L. Dietz, D. Northcutt, J. Stenson, K. van den Wymelenberg. Evaluation of a bioaerosol sampler for indoor environmental surveillance of Severe Acute Respiratory Syndrome Coronavirus 2. *PLoS One.* **16** (2021) e0257689.
9. Y. Liu *et al.*, Stability of SARS-CoV-2 on environmental surfaces and in human excreta. *J. Hosp. Infect*. **107** (2021) 105.
10. H. William, H. Syracuse and R. J. Hennick Cayuga, STERILIZATION APPARATUS, Patent Number USOO82O3124B2, Date of Patent Jun. 19, (2012). https://patentimages.storage.googleapis.com/c6/c0/23/f64038027aa4ed/US8203124.pdf.
11. C. E. Hunter, D. G. Narayan, L. E. McNeil, and J. H. Hebrank, METHODS AND APPARATUS FOR ULTRAVOLET STERILIZATION, Number patent US 2006O147339A1, Date of Patent Jul. 6, 2006. https://patents.google.com/patent/US20060147339A1/en?q=(sterilization+apparatus+uv)&oq=sterilization+apparatus+uv.
12. Report for analysis, Guangdong detection center of microbiology, number report 2020FM05977R01E, verification code 30921548, www. gddcm.com.
13. G. Kampf *et al*., Persistence of coronaviruses on inanimate surfaces and their inactivation with biocidal agents. *Journal of hospital infection* **104** (2020) 246-251.
14. K. Wang *et al.*, Risk of air and surface contamination of SARS-CoV-2 in isolation wards and its relationship with patient and environmental characteristics. *Ecotoxicol Environ Saf.* **241** (2022) 113740. https://doi.org/10.1016/j.ecoenv.2022.113740.
15. G. Correia *et al*., SARS-CoV-2 air and surface contamination in residential settings. *Sci Rep.* **12** (2022) 18058. 10.1038/s41598-022-22679-y.

16. X. Zhang *et al.,* Monitoring SARS-CoV-2 in air and on surfaces and estimating infection risk in buildings and buses on a university campus. *J Expo Sci Environ Epidemiol*. **32** (2022) 751-758. 10.1038/s41370-022-00442-9.

17. J. Biryukov *et al*., Increasing Temperature and Relative Humidity Accelerates Inactivation of SARS-CoV-2 on Surfaces. *mSphere.* (2020) 5.

18. A. Kratzel *et al*., Temperature-dependent surface stability of SARS-CoV-2. *J Infect.* **81** (2020) 452-82.

19. N. Van Doremalen *et al*., Aerosol and Surface Stability of SARS-CoV-2 as Compared with SARS-CoV-1. *N Engl J Med.* **382** (2020) 1564-7.

20. E. M. Durán-Manuel *et al*., Clonal dispersion of Acinetobacter baumannii in an intensive care unit designed to patients COVID-19. *J Infect Dev Ctries.* **15** (2021) 58-68.

21. E. K. Jeong, J. E. Bae, and I. S. Kim, Inactivation of influenza A virus H1N1 by disinfection process. *Am J Infect. Control*. **38** (2010) 354-60.

22. J. Choi, M. Lee, Y. Lee, Y. Song, Y. Cho, and T. Lim, Effectiveness of Plasma-Treated Hydrogen Peroxide Mist Disinfection in Various Hospital Environments. *Int J Environ Res Public Health.* **18** (2021) 9841.

23. V. Monzillo *et al.*, Ozonized Gel Against Four Candida Species A Pilot Study and Clinical Perspectives. *Materials.* (2020) 13.

24. G. Franke *et al*., An automated room disinfection system using ozone is highly active against surrogates for SARS-CoV-2. *J Hosp Infect.* **112** (2021) 108-13.

25. T. L. Wiemken *et al*., Evaluation of the effectiveness of improved hydrogen peroxide in the operating room. *Am J Infect Control*. **42** (2014) 1004-5.

26. A. Darge, A. G. Kahsay, H. Hailekiros, S. Niguse, and M. Abdulkader, Bacterial contamination and antimicrobial susceptibility patterns of intensive care units medical equipment and inanimate surfaces at Ayder Comprehensive Specialized Hospital, Mekelle, Northern Ethiopia. *BMC Res Notes*. (2019) 12.

27. G. Kac *et al*., Evaluation of a new disinfection procedure for ultrasound probes using ultraviolet light. *J Hosp Infect.* **65** (2007) 163-8.

28. J. M. Jennings *et al.*, A back table ultraviolet light decreases environmental contamination during operative cases. *Am J Infect Control*. (2021) S0196-6553(21)00640-4.

29. T. E. Meawed, S. M. Ahmed, S. M. S. Mowafy, G.M. Samir and R. H. Anis, Bacterial and fungal ventilator associated pneumonia in critically ill COVID-19 patients during the second wave. *J Infect Public Health.* **14** (2021) 1375-80.

30. `https://Www.Conbioetica.Mexico.Salud.Gob.Mx/Descargas/Pdf/Normatividad/Normatinacional/10._NAL._Reglamento_de_Investigacion.Pdf`.

31. T. Liu, Digital-Output Relative Humidity & Temperature Sensor/Module DHT22 (DHT22 Also Named as AM2302) Capacitive-Type Humidity and Temperature Module/Sensor.

32. M. A. Cureño-Díaz *et al*., Impact of the modification of a cleaning and disinfection method of mechanical ventilators of COVID-19 patients and ventilator-associated pneumonia One year of experience. *Am J Infect Control*. **49** (2021) 1474-80.

33. J. Rodríguez-Baño *et al*., Biofilm Formation in Acinetobacter baumannii Associated Features and Clinical Implications. *Clin Microbiol Infect* **14** (2008) 276-278

34. M. Gulati *et al*., In Vitro Culturing and Screening of Candida albicans Biofilms. *Curr Protoc Microbiol* (2018) 50

35. G. Ibáñez-Cervantes *et al*., Ozone as an Alternative Decontamination Process for N95 Facemask and Biosafety Gowns. *Mater Lett* (2022) 311

36. S. M. Hirabara *et al*., SARS-COV-2 Variants Differences and Potential of Immune Evasion. *Front Cell Infect Microbiol.* **11** (2022) 1401.

37. A. Rouzé and S. Nseir Hospital-Acquired Pneumonia/Ventilator-Associated Pneumonia and Ventilator-Associated Tracheobronchitis in COVID-19. *Semin Respir Crit Care Med.* **43** (2022) 243-247.

38. B. Kayaaslan *et al*., Incidence and risk factors for COVID-19 associated candidemia (CAC) in ICU patients. *Mycoses.* **65** (2022) 508-516

39. M. Biasin, *et al*., UV-C irradiation is highly effective in inactivating SARS-CoV-2 replication. *Scientific Reports* **11** (2021) 6260. https //doi.org/10.1038/s41598-021-85425-w

40. R. T. Robinson *et al*., UV222 disinfection of SARS-CoV-2 in solution. *Scientific Reports* **12** (2022) 14545. https //doi.org/10.1038/s41598-022-18385-4

41. B. Ma, P. M. Gundy, C. P. Gerba, M. D. Sobsey, and K. G. Linden, UV Inactivation of SARS-CoV-2 across the UVC Spectrum KrCl* Excimer, Mercury-Vapor, and Light-Emitting-Diode (LED) Sources. *Appl Environ Microbiol.* (2021) 87.

42. S. J. Boegel *et al*., Robust Evaluation of Ultraviolet-C Sensitivity for SARS-CoV-2 and Surrogate Coronaviruses. *Microbiol Spectr.* (2021) 9.

43. C. Russo *et al*., Effect of a UV-C Automatic Last-Generation Mobile Robotic System on Multi-Drug Resistant Pathogens. *Int J Environ Res Public Health*. (2021) 18.

44. L. Hazell, F. Allan, A. M. Emery, and M. R. Templeton, Ultraviolet disinfection of Schistosoma mansoni cercariae in water. *PLOS Negle Trop Dis.* **15** (2021) e0009572.

45. S. Debnath, Low Cost Homemade System to Disinfect Food Items from SARS-CoV-2. *J Med Syst.* (2020) 44.

46. S. H. Rakib *et al.*, Design and Development of a low cost Ultraviolet Disinfection system to reduce the cross infection of SARS-CoV-2 in ambulances. Proceedings of International Conference on Electronics, *Communications and Information Technology*, ICECIT (2021).

47. G. Zhang *et al.*, Ultraviolet Light-Degradation Behavior and Antibacterial Activity of Polypropylene/ZnO Nanoparticles Fibers. *Polymers* **11** (2019) 1841

48. M. Raeiszadeh, and B. Adeli, A Critical Review on Ultraviolet Disinfection Systems against COVID-19 Outbreak Applicability, Validation, and Safety Considerations. *ACS Photonics.* **7** (2020) 2941-51.

49. H. Mamane-Gravetz, K. G. Linden, A. Cabaj, and R. Sommer Spectral sensitivity of Bacillus subtilis spores and MS2 coliphage for validation testing of ultraviolet reactors for water disinfection. *Environ Sci Technol* **39** (2005) 7845-7852

50. F. Barancheshme, J. Philibert, Noam-Amar N, Y. Gerchman and B. Barbeau, Assessment of saliva interference with UV-based disinfection technologies. *J Photochem Photobiol B Biol*, **217** (2021) 112168

51. H. Y. Buse, J. S. Hall, G. L. Hunter, and J. A. Goodrich, Differences in UV-C LED Inactivation of Legionella pneumophila Serogroups in Drinking Water. *Microorganisms.* **10** (2022) 352.

52. A. Argyraki *et al*., UV light assisted antibiotics for eradication of in vitro biofilms. *Sci Rep.* **8** (2018) 1-9.

53. C. B. Lineback, C. A. Nkemngong, S. T. Wu, X. Li, P. J. Teska, H. F. Oliver, Hydrogen Peroxide and Sodium Hypochlorite Disinfectants Are More Effective against Staphylococcus aureus and Pseudomonas aeruginosa Biofilms than Quaternary Ammonium Compounds. *Antimicrob Resist Infect Control* **7** (2018) 1-7.